μg of steroid each were prepared and implanted as in (*2*).
4. B. S. McEwen, P. G. Davis, B. Parsons, D. W. Pfaff, *Annu. Rev. Neurosci.* **2**, 65 (1979).
5. These pellets were directed at the mediobasal hypothalamus (MBH) and contained [2,4,6,7,-^{3}H(N)]E_2 diluted with E_2 to a specific activity of 1.69 mCi/mole. Nine extracted pellets contained 1.68 ± 0.11 μg of E_2. The pups were killed 24 hours after implantation and their brains were removed, frozen, and hemisected. After the implants were retrieved, MBH samples from each hemisection were digested and radioactivity was measured. Background values of vials without tissue were subtracted before the disintegrations per minute were converted to nanograms of E_2. Retrieved pellets contained 187.9 ± 67.6 ng of E_2. Implanted MBH samples contained 4.4 to 10.0 ng of E_2 (mean = 6.8 ± 0.7. No E_2 was detected in the contralateral MBH in five pups; in the other three pups, the contralateral MBH contained 0.6, 0.8, and 1.4 ng of E_2.
6. C. A. Barraclough and R. A. Gorski, *Endocrinology* **68**, 68 (1961).
7. Ten days after ovariectomy, females were injected subcutaneously with 2 μg of EB per day for 2 days. The next day, they received 500 μg of progesterone subcutaneously 4 hours before testing. They were retested 4 days later after receiving more EB (2 μg/day for 3 days) and progesterone (500 μg 4 hours before the test). Each female was mounted ten times per test (LQ = lordosis frequency × 10).
8. M. J. Baum and J. T. M. Vreeburg, *Science* **182**, 283 (1973).
9. Six days after tests of female sexual behavior, females received 2 μg of EB plus 200 μg of DHTP subcutaneously daily for 16 days and were tested for male sexual behavior on days 7, 12, and 16. Two weeks later, they received 2 μg of EB per day subcutaneously for 12 days and were tested on days 7 and 12. Tests lasted 30 minutes. Mounts with pelvic thrusting and intromission patterns were scored. Intromission patterns were infrequent and did not differ between groups.
10. Brains were sectioned and stained as in (*11*). Camera-lucida drawings of the part of the POA that stained as darkly as the suprachiasmatic nuclei were retraced on a digitizing tablet that computed their areas. The SDN volume is the sum of the areas (corrected for magnification) × 60 μm (section thickness).
11. R. A. Gorski, J. H. Gordon, J. E. Shryne, A. M. Southam, *Brain Res.* **148**, 333 (1978).
12. The LQ's were averaged across tests for each female. Mean LQ's of females with implants in the same hypothalamic region were compared by using a one-way analysis of variance. If the groups (E_2 left, E_2 right, and control) differed significantly overall, specific comparisons were made by the Newman-Keuls procedure.
13. All data in the text and graphs are given as means ± standard errors.
14. Mount frequencies and latencies were analyzed as described in (*12*).
15. One female died before the EB tests began.
16. M. C. Corballis and M. J. Morgan, *Behav. Brain Sci.* **1**, 261 (1978).
17. J. Weisz and I. I. Ward, *Endocrinology* **106**, 306 (1980); J. D. Wilson, F. W. George, J. E. Griffin, *Science* **211**, 1278 (1981).
18. L. W. Clemens, B. A. Gladue, L. P. Coniglio, *Horm. Behav.* **10**, 40 (1978); R. L. Meisel and I. L. Ward, *Science* **213**, 239 (1981).
19. L. W. Clemens and B. A. Gladue, *Horm. Behav.* **11**, 190 (1978); B. A. Gladue and L. G. Clemens, *Endocrinology* **103**, 1702 (1978).
20. P. G. Davis, B. S. McEwen, D. W. Pfaff, *ibid.* **104**, 898 (1979).
21. L. J. Pellegrino, A. S. Pellegrino, A. J. Cushman, *A Stereotaxic Atlas of the Rat Brain* (Plenum, New York, 1979), p. 102.
22. Abbreviations: AHA, anterior hypothalamic area; AM, anteromedial nucleus of the thalamus; ARH, arcuate nucleus of the hypothalamus; CAa, anterior commissure, anterior part; CAp, anterior commissure, posterior part; CP, posterior commissure; DBB, diagonal band of Broca; DMH, dorsomedial nucleus of the hypothalamus; FX, fornix; HP, habenula-interpeduncular tract; OT, optic tract; PF, parafascicular nucleus of the thalamus; PH, posterior nucleus of the hypothalamus; PM, mammillary peduncle; PMD, dorsal premammillary nucleus; PMV, ventral premammillary nucleus; SC, suprachiasmatic nucleus; and TUO, olfactory tubercle.
23. This research was supported by grant MH 26481 from the National Institute of Mental Health and was submitted by E.J.N. in partial fulfillment of the requirements for the Ph.D. We thank R. Robertson and C. Ribak for use of the camera lucida. We thank Plenum Press and L. Pellegrino for permission to reproduce the atlas section shown in Fig. 1A.

28 January 1982; revised 9 July 1982

Mapping the Primate Visual System with [2-^{14}C]Deoxyglucose

Abstract. *The [2-^{14}C]deoxyglucose method was used to identify the cerebral areas related to vision in the rhesus monkey (*Macaca mulatta*). This was achieved by comparing glucose utilization in a visually stimulated with that in a visually deafferented hemisphere. The cortical areas related to vision included the entire expanse of striate, prestriate, and inferior temporal cortex as far forward as the temporal pole, the posterior part of the inferior parietal lobule, and the prearcuate and inferior prefrontal cortex. Subcortically, in addition to the dorsal lateral geniculate nucleus and superficial layers of the superior colliculus, the structures related to vision included large parts of the pulvinar, caudate, putamen, claustrum, and amygdala. These results, which are consonant with a model of visual function that postulates an occipito-temporo-prefrontal pathway for object vision and an occipito-parieto-prefrontal pathway for spatial vision, reveal the full extent of those pathways and identify their points of contact with limbic, striatal, and diencephalic structures.*

Many structures involved in processing visual information in the monkey have been identified through the combined use of neurobehavioral, electrophysiological, and anatomical techniques. Converging evidence has revealed a sequential pathway for processing information about visual objects that begins with retino-geniculate input to the striate cortex, proceeds through the prestriate cortex, and continues along a corticocortical route to the inferior temporal and then the inferior prefrontal cortex (*1, 2*). Classical mapping techniques have also identified another cortical visual pathway, which again begins with retino-geniculate input to the striate cortex but appears to be specialized for processing information about visual space; the corticocortical route in this case is through the prestriate, posterior parietal, and prearcuate cortex (*1, 3, 4*). Both pathways receive projections from the superior colliculus via the pulvinar and send projections to various limbic, striatal, and diencephalic structures. Despite a range of research efforts, however, the full extent of these two cortical pathways and their exact subcortical targets remain undefined. In the studies described here we used the [2-^{14}C]deoxyglucose (*5*) method to measure local cerebral glucose utilization (LCGU). This method enabled us to prepare a comprehensive map of the functioning visual system in a single preparation (*6*).

Four rhesus monkeys (*Macaca mulatta*) weighing 2.5 to 4.5 kg were subjected to unilateral (right) section of the optic tract about 6 weeks before we measured the LCGU. Metabolic activity produced by direct retinal stimulation was thereby limited to one hemisphere, and it was thus possible to compare LCGU in a "seeing" and a "blind" hemisphere in the same animal (*7*).

On the day of the experiment each monkey was lightly anesthetized with halothane and nitrous oxide, catheters for deoxyglucose administration and blood sampling were inserted into the femoral vessels, and the animal was seated in a primate chair. After at least 4 hours of recovery from anesthesia, the monkey was placed within an encircling screen, which displayed a brightly illuminated, high-contrast geometric pattern that rotated counterclockwise at 5 to 7 rev/min. The monkey focused its gaze on this visual stimulus throughout most of the experimental session, tracking it with head and eye movements. To begin the experiment we gave an intravenous injection of [2-^{14}C]deoxyglucose (100 μCi/kg). Forty-five minutes later the animal was killed, and the brain was removed, frozen, and prepared for quantitative autoradiography. Other details of the method have been described (*5, 8*).

The hemispheric differences that we found in optical density (see Fig. 1) reflected only the relative rates of glucose utilization. To quantify the rates we used a computerized image-processing system which, supplied with the plasma variables monitored during the experiment and the kinetic constants for the species (*5*), transform the autoradiographs into color-coded maps of the actual LCGU values (*9*). Determination of the LCGU values for every structure identified in Fig. 1 was based on readings of areas 2 to 3 mm square at all of the points indicated. In Table 1, the structures are categorized as "visual" or "nonvisual" on the basis of the presence or absence of a statistically significant degree of hemi-

0036-8075/82/1022-0394$01.00/0

spheric asymmetry across the four animals (*10*).

In Fig. 1, sections P20 and P13 show conspicuous hemispheric asymmetry throughout striate and prestriate cortex, areas OC, OB, and OA (*11*). The more rostral sections (P5 through A20) reveal the tissue belonging to the ventral cortical visual pathway, known to be critical for object vision (*2*). Clear side-to-side differences occur throughout the inferior temporal cortex, areas TEO and TE; the ventral portion of the temporal pole, area TG_v; the fusiform gyrus, area TF; and in portions of the upper bank of the superior temporal sulcus. The limits of this visual tissue are marked by sharp changes in density both on the ventral surface of the temporal lobe and within the upper bank of the superior temporal sulcus. Beyond the temporal lobe hemispheric asymmetry occurred in the inferior part of the prefrontal cortex, area FD_v (A30, not shown). These hemispheric differences in LCGU were greatest within the striate cortex, moderate within the prestriate and posterior temporal cortex, and least in the anterior portion of inferior temporal and inferior prefrontal cortex (see Table 1). Metabolic asymmetry in the temporal lobe did not extend anteromedially beyond the ventral portion of area TG into the hippocampal gyrus, area TH (A5, A10), or the entorhinal or piriform cortices (A15, A20). Nor did it extend into the primary auditory cortex, area TC (P1, A5, A10); the superior temporal gyrus, area TA (P5 through A20); or the insula, areas IB and IA (A10, A15).

Subcortically, areas of depressed LCGU in the blind hemisphere were found in structures known to receive direct inputs from the ventral cortical visual pathway (*12, 13*). Within the temporal lobe, side-to-side differences in LCGU could be seen in the lateral and basolateral but not the basal accessory nuclei of the amygdala (Fig. 1, A15), posteroventral but not posterodorsal or anterior putamen (A5 through A20), ventral but not dorsal claustrum (A5 through A20), and the tail of the caudate nucleus (P1, A5, A10). The other major subcortical temporal lobe structure, the hippocampal formation, showed hemispheric symmetry throughout (P1, A5, A10). Within the frontal lobe, hemispheric differences were observed in the anterior part of the head of the caudate nucleus (A23, not shown). Except for the ventral claustrum, all of the subcortical areas that were functionally depressed in the blind hemisphere have been implicated in visual discrimination learning and memory on the basis of neurobehavioral studies (*14*).

Dorsally within the cortex, the autoradiographs also revealed the tissue belonging to the second cortical visual pathway, believed to be specialized for spatial vision (*3*). In Fig. 1, the posterior portion of the inferior parietal lobule, area PG, shows distinct hemispheric asymmetry (P1), the limits of which are marked by sharp changes in density both on the lateral surface and on the upper bank of the intraparietal sulcus. More anteriorly, side-to-side differences occur in the prearcuate region of the frontal cortex, area FD_Δ, the site of the frontal eye fields (A20). Both the body (A10) and the posterior portion of the head of the caudate nucleus (A15, A20), known to receive anatomical input from posterior parietal and prearcuate frontal cortex, respectively (*13*), show small but statistically significant left-right differences in LCGU. The hemispheric difference found cortically in the posterior portion of the inferior parietal lobule did not extend into the anterior portion of the lobule, area PF (A5), or into the superior parietal lobule, area PE (P5, P1). Likewise, the hemispheric difference in the prearcuate cortex did not extend posteri-

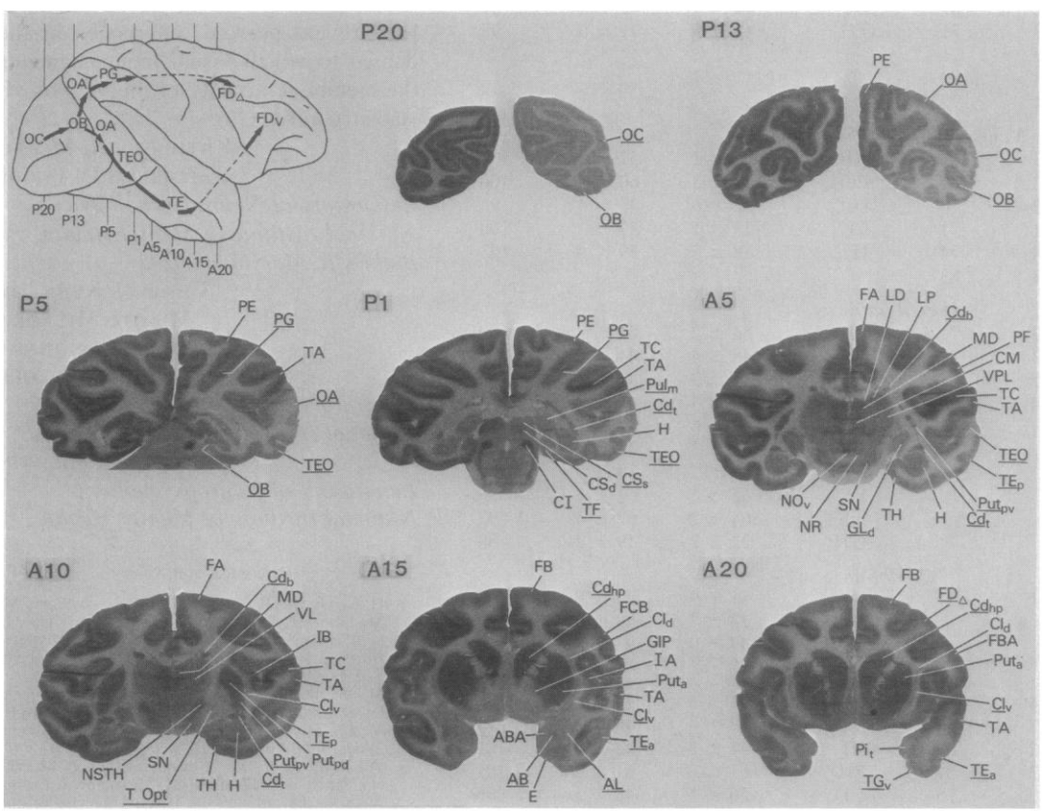

Fig. 1. [2-^{14}C]Deoxyglucose autoradiographs from a representative monkey, prepared with a right optic tract section and a forebrain commissurotomy (*7*), showing relative rates of glucose utilization (the darker the region the higher the rate). The designations P20 through A20 refer to the coronal level of the section in millimeters posterior (P) or anterior (A) to the interaural plane. Structures related to vision are revealed by their depressed metabolic activity in the "blind" right hemisphere compared to the "normal" left hemisphere. Every structure identified here is listed in Table 1, where it is categorized as either visual or nonvisual on the basis of statistical analysis. The visual structures, both cortical and subcortical, are underlined in the figure and discussed in the text in relation to the two cortical visual pathways schematized in the diagram in the upper left. Anatomical connections among the cortical visual areas, both within and between the two systems, are not limited to those shown. For abbreviations, see (*21*).

orly into the premotor or motor cortex, areas FA, FB, FCB, or FBA (A10, A15, A20). Nor were left-right differences found in any subcortical structures known to be related to the motor system, such as the red nucleus, substantia nigra, subthalamic nucleus, and the globus pallidus (A5, A10, A15).

The distinction between visual and motor systems was present even within visuomotor structures. Within the midbrain, there were clear left-right differences between the superficial layers of the superior colliculi, whereas the intermediate and deep layers showed symmetrical activity (P1). These results are in accord with previously established functional divisions based on electrophysiological findings (*15*). Metabolic symmetry was likewise observed in the oculomotor nucleus (A5).

Asymmetries within the diencephalon were present in the optic tract (A10) and dorsal lateral geniculate body (A5), as well as in the lateral and inferior pulvinar (A2, not shown), nuclei that receive input both from visual cortical areas and from the superficial layers of the superior colliculus (*16*). The medial pulvinar also differed significantly side-to-side, suggesting that it too participates in visual function (P1). In contrast, nucleus lateralis posterior, considered in some species to be part of the pulvinar complex (*17*) but which receives mainly from the deep layers of the superior colliculus (*18*), showed no such difference. All other thalamic nuclei that were chosen for analysis as representatives of nonvisual structures showed symmetrical metabolic activity. These included the medial geniculate body (A3, not shown) and the nuclei ventralis posterolateralis, ventralis lateralis, medialis dorsalis, lateralis dorsalis, and centrum medianum (A5).

The [2-^{14}C]deoxyglucose method revealed within a single preparation all cerebral areas that are strongly activated by retinal stimulation. The simultaneous visualization of these areas emphasizes the profound impact of vision on the activity of the cerebral hemispheres. The present results contribute to our understanding of the visual system in three ways. First, they provide a more complete inventory of the structures that participate in visual processing, including, for example, temporal cortical tissue beyond the inferior convexity and subcortical structures such as the medial pulvinar and large portions of the body of the caudate nucleus. Second, within each structure, they reveal the full extent of the tissue that is visual in function, thereby permitting delineation of the visual-nonvisual borders (*19*). And third, they reveal marked differences in the degree to which visual input augments the metabolic activity of the various visual structures (*20*).

Table 1. Means and standard errors of LCGU values in micromoles per 100 grams per minute in the normal and blind hemispheres of four animals. For all the structures categorized as "visual," LCGU in the blind hemisphere is significantly less than that in the normal hemisphere (OC_{iv}, OB, TEO, FD_v, CS_s = $P < .001$; TF, TG_v, AB, Put_{pv}, Cd_{ha}, Cd_{hp}, Cd_b = $P < .05$; all others = $P < .01$). The LCGU in the blind hemisphere is also expressed as a percentage of the normal hemisphere (that is, blind/normal × 100). Visual structures and nearby nonvisual structures are grouped according to their description in the text. See (*21*) for abbreviations.

"Visual" structures				"Nonvisual" structures			
Area	Normal	Blind	Normal (%)	Area	Normal	Blind	Normal (%)
			Ventral pathway: Cortical				
OC_{iv}	101 ± 7	30 ± 4	30	E	34 ± 5	32 ± 3	93
OC_{-iv}	50 ± 4	22 ± 3	44	Pi_t	33 ± 2	32 ± 2	99
OB	61 ± 1	33 ± 2	54	TC	80 ± 4	79 ± 4	99
OA	59 ± 3	41 ± 3	70	TA	55 ± 3	56 ± 4	103
TEO	58 ± 3	35 ± 3	60	IB	57 ± 5	61 ± 4	107
TE_p	53 ± 3	35 ± 2	67	IA	44 ± 4	45 ± 4	101
TE_a	48 ± 2	35 ± 3	71	TH	43 ± 5	41 ± 6	97
TF	53 ± 7	37 ± 9	71				
TG_v	40 ± 4	32 ± 4	80				
FD_v	75 ± 3	54 ± 4	72				
			Ventral pathway: Subcortical				
AL	48 ± 2	32 ± 3	68	ABA	31 ± 2	31 ± 2	100
AB	42 ± 3	27 ± 2	66	Put_{Pd}	60 ± 3	60 ± 3	100
Put_{pv}	54 ± 4	37 ± 2	70	Put_a	52 ± 6	49 ± 4	95
Cl_v	27 ± 1	19 ± 1	71	Cl_d	23 ± 1	23 ± 1	100
Cd_t	53 ± 6	39 ± 4	74	H	38 ± 3	39 ± 4	103
Cd_{ha}	58 ± 1	48 ± 1	83				
			Dorsal pathway				
PG	66 ± 4	47 ± 3	71	PE	54 ± 2	54 ± 2	100
FD_Δ	54 ± 3	45 ± 3	83	PF	48 ± 4	44 ± 5	92
Cd_b	58 ± 4	45 ± 5	78	FA	47 ± 2	49 ± 1	103
Cd_{hp}	56 ± 4	50 ± 4	90	FB	40 ± 3	42 ± 2	104
				FCB	60 ± 6	54 ± 5	90
				FBA	44 ± 3	45 ± 4	101
				NR	39 ± 7	39 ± 7	100
				SN	55 ± 5	53 ± 5	97
				NSTH	64 ± 2	59 ± 4	92
				G1P	22 ± 2	19 ± 2	88
			Midbrain				
CS_s	72 ± 4	36 ± 1	51	CS_d	51 ± 9	47 ± 8	93
				NO_v	72 ± 7	68 ± 6	94
				CI	99 ± 9	97 ± 8	99
			Diencephalon				
T Opt	33 ± 3	17 ± 4	52	GM	81 ± 6	79 ± 6	98
GL_d	51 ± 7	33 ± 7	66	VPL	47 ± 4	46 ± 3	97
Pul_i	49 ± 2	31 ± 2	63	VL	41 ± 2	42 ± 2	101
Pul_l	42 ± 4	34 ± 3	81	MD	61 ± 3	61 ± 2	101
Pul_m	43 ± 3	33 ± 3	75	LD	50 ± 5	48 ± 5	96
				CM	46 ± 6	46 ± 6	100
				LP	47 ± 3	45 ± 1	96

KATHLEEN A. MACKO
CHARLENE D. JARVIS
Laboratory of Neuropsychology, National Institute of Mental Health, Bethesda, Maryland 20205
CHARLES KENNEDY
MIKOTO MIYAOKA
MAMI SHINOHARA
LOUIS SOKOLOFF
Laboratory of Cerebral Metabolism, National Institute of Mental Health
MORTIMER MISHKIN
Laboratory of Neuropsychology, National Institute of Mental Health

References and Notes

1. H. G. J. M. Kuypers, M. K. Szwarcbart, M. Mishkin, H. E. Rosvold, *Exp. Neurol.* **11**, 245 (1965); D. N. Pandya and H. G. J. M. Kuypers, *Brain Res.* **13**, 13 (1969); E. G. Jones and T. P. S. Powell, *Brain* **93**, 793 (1970).
2. M. Mishkin, in *Brain and Human Behavior*, A. G. Karczmar and J. C. Eccles, Eds. (Springer-Verlag, Berlin, 1972), pp. 187–208; C. E. Rosenkilde, *Behav. Neural Biol.* **25**, 301 (1975).
3. W. Pohl, *J. Comp. Physiol. Psychol.* **82**, 227 (1973); H. Barbas and M-M. Mesulam, *J. Comp. Neurol.* **200**, 407 (1981); L. G. Ungerleider and M. Mishkin, in *The Analysis of Visual Behavior*, D. J. Ingle *et al.*, Eds. (MIT Press, Cambridge, Mass., 1982), p. 485.

4. V. B. Mountcastle, J. C. Lynch, A. Georgopolous, H. Sakata, C. Acuna, *J. Neurophysiol.* **38**, 871 (1975); D. L. Robinson, M. E. Goldberg, G. B. Stanton, *ibid.* **41**, 910 (1978).
5. L. Sokoloff, M. Reivich, C. Kennedy, M. H. DesRosiers, C. S. Patlak, K. D. Pettigrew, O. Sakurada, M. Shinohara, *J. Neurochem.* **28**, 897 (1977); C. Kennedy, O. Sakurada, M. Shinohara, J. Jehle, L. Sokoloff, *Ann. Neurol.* **4**, 293 (1978).
6. For preliminary reports of this work, see C. Kennedy, C. D. Jarvis, O. Sakurada, M. Mishkin, *Neurology* **28**, 366 (1978); and C. D. Jarvis, M. Mishkin, M. Shinohara, O. Sakurada, M. Miyaoka, C. Kennedy *Soc. Neurosci. Abstr.* **4**, 632 (1978).
7. In two of the animals the tract section was combined with section of the corpus callosum and anterior commissure. Although the addition of commissurotomy reduced LCGU in certain visual structures of the blind hemisphere more than optic tract section alone, it did not reveal any additional visual structures [K. A. Macko, M. Miyaoka, C. Kennedy, L. Sokoloff, M. Mishkin, *Soc. Neurosci. Abstr.* **6**, 671 (1980)].
8. C. Kennedy, M. H. DesRosiers, O. Sakurada, M. Shinohara, M. Reivich, J. W. Jehle, L. Sokoloff, *Proc. Natl. Acad. Sci. U.S.A.* **73**, 4230 (1976).
9. C. Goochee, W. Rasband, L. Sokoloff, *Ann. Neurol.* **7**, 359 (1980).
10. No structures examined in control monkeys (optic tracts intact) tested under the same conditions have shown hemispheric asymmetry (M. Ito and C. Kennedy, unpublished data; K. A. Macko, unpublished data).
11. Cytoarchitectonic designations are those of G. von Bonin and P. Bailey [*The Neocortex of* Macaca mulatta (Univ. of Illinois Press, Urbana, 1947)].
12. A. G. Herzog and G. W. Van Hoesen, *Brain Res.* **115**, 57 (1976); T. N. Johnson, H. E. Rosvold, M. Mishkin, *Exp. Neurol.* **21**, 20 (1968); B. Turner, M. Mishkin, M. Knapp, *J. Comp. Neurol.* **191**, 515 (1980); G. W. Van Hoesen, E. H. Yeterian, R. Lavisso-Mourey, *ibid.* **199**, 205 (1981); D. G. Whitlock and D. J. H. Nauta, *ibid.* **106**, 183 (1956).
13. J. M. Kemp and T. P. S. Powell, *Brain* **93**, 525 (1970).
14. A. A. Buerger, C. G. Gross, C. E. Rocha-Miranda, *J. Comp. Physiol. Psychol.* **86**, 440 (1974); I. Divac, H. E. Rosvold, M. K. Szwarcbart, *ibid.* **63**, 184 (1967); E. T. Rolls, in *Brain Mechanisms of Sensation*, M. Sata and R. Norgren, Eds. (Academic Press, New York, 1980), pp. 1–47; B. J. Speigler and M. Mishkin, *Behav. Brain Res.* **3**, 303 (1981).
15. Cells within the superficial layers discharge primarily to visual stimuli, while cells in the deeper layers discharge mainly in relation to eye movements [R. H. Wurtz and J. E. Albano, *Annu. Rev. Neurosci.* **3**, 189 (1980)].
16. M. Ogren and A. Hendrickson, *Exp. Neurol.* **53**, 780 (1976); L. G. Ungerleider, T. W. Galkin, M. Mishkin, *Soc. Neurosci. Abstr.* **6**, 481 (1980).
17. J. K. Harting, W. C. Hall, I. T. Diamond, *Brain, Behav. Evol.* **6**, 424 (1972).
18. L. A. Benevento and J. H. Fallon, *J. Comp. Neurol.* **160**, 339 (1975).
19. K. Macko, C. Kennedy, L. Sokoloff, M. Mishkin, *Soc. Neurosci. Abstr.* **7**, 832 (1981).
20. For example, activity in the visually stimulated compared to the visually deafferented hemisphere is more than 200 percent greater in layer IV of area OC, 100 percent greater in the superficial layer of the superior colliculus, but only 50 percent greater in the dorsal lateral geniculate nucleus. The latter value is about the same as the value not only in area TE, another exclusively visual structure, but also in area PG, known to be a polysensory area. These differences in the quantitative contribution of visual input to the metabolic activity of the various structures related to vision have no known explanation at present and therefore pose an intriguing new question for future research.
21. Abbreviations used: AB, basal nucleus of the amygdala; ABA, basal accessory nucleus of the amygdala; AL, lateral nucleus of the amygdala; Cd, caudate nucleus (b, body; ha, anterior part of head; hp, posterior part of head; t, tail); CI, inferior colliculus; Cl, claustrum (d, dorsal part; v, ventral part); Cm, nucleus (N.) centrum medianum; CS, superior colliculus (d, deep layers; s, superficial layers); E, entorhinal cortex; FA, precentral cortex; FB, dorsal precentral cortex; FBA, posteroventral premotor cortex; FCB, anteroventral premotor cortex; FD_{α}, posterior prefrontal cortex; GlP, globus pallidus; GL, corpus geniculatum laterale (d, dorsal); GM, corpus geniculatum mediale; H, hippocampal formation; IA, anterior insular cortex; IB, posterior insular cortex; LD, N. lateralis dorsalis; LP, N. lateralis posterior; MD, N. medialis dorsalis; NO, N. occulomotorii; NR, N. ruber; NSTH, N. subthalamicus; OA, anterior prestriate cortex; OB, posterior prestriate cortex; OC_{IV}, layer IV of striate cortex; OC_{-IV}, striate cortex, excluding layer IV; PE, superior parietal cortex; PF, anterior inferior parietal cortex; PG, posterior inferior parietal cortex; Pi, piriform cortex (t, temporal); Pul, N. pulvinaris (i, inferior; m, medial; l, lateral); Put, putamen (a, anterior; p, posterior); SN, substantia nigra; TA, superior temporal cortex, lateral surface; TC, superior temporal cortex, supratemporal plane; TE, anterior inferior temporal cortex (a, anterior; p, posterior); TEO, posterior inferior temporal cortex; TF, fusiform cortex; TG, temporal polar cortex (v, ventral); TH, parahippocampal cortex; T Opt, optic tract; VL, N. ventralis lateralis; VPL, N. ventralis posterolateralis.

2 March 1982; revised 25 June 1982

Pigeon Perception of Letters of the Alphabet

Abstract. *In a three-choice discrimination task three pigeons learned to distinguish each letter of the alphabet from all other letters. Errors during learning were based on 54 presentations of each target letter with every other letter. The errors were used to scale letters in a multidimensional similarity space and to associate them in hierarchical clusters. The results resembled those generated from similarity judgments by humans, suggesting cross-task and cross-species generality in processes of letter discrimination.*

Does the world look the same to pigeons and people? Herrnstein and coworkers (*1*) found that pigeons can identify categories such as "tree" and "fish" in photographs. However, the perception of such complex and variable stimuli is difficult to analyze. The birds in the present experiment learned instead the letters of the alphabet. These relatively simple stimuli yielded similarity patterns that are well correlated with comparable data for human subjects. The method may be useful in further studies of form perception in animals.

Each pigeon was placed in a box with a small television monitor screen set in one wall. On this screen an Atari home computer generated black letters on a white ground. The letters were formed within a five by seven dot matrix 2.0 mm wide and 2.8 mm high and were of the same format as those used by Podgorny and Garner (*2*) in a recent study of letter perception in humans. Three letters appeared in each experimental trial; they were horizontally aligned and spaced 2.3 cm apart, each behind a key made from a glass microscope slide.

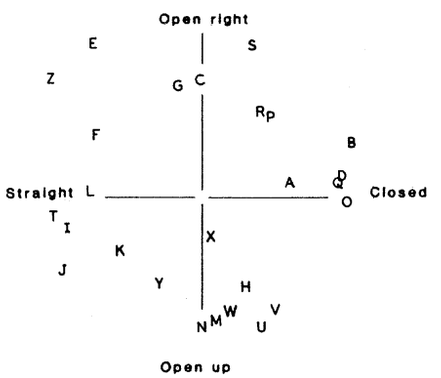

Fig. 1. Two-dimensional representation by ALSCAL of the similarity of letters perceived by the pigeons. In general, where two letters are far apart, the pigeon made few errors when discriminating them; where two letters are close together, it made many errors. Ideally, the closest pair would have the most errors, the next closest the next most, and so on. The names near the dimensional extremes call attention to common features of nearby letters.

Three white Carneaux pigeons were trained by standard methods to eat from a feeder located below and to the left of the display screen and to peck at randomly selected single letters appearing behind any of the three response keys. In the test procedure the bird was rewarded for pecking at a single letter—the target letter—on four successive daily sessions. This letter appeared equally often behind each of the glass keys on 675 test trials each day, while one of the other letters appeared behind both of the other keys. Each of the 25 nontarget letters appeared on one trial in each successive block of 25 trials. If the target letter was pecked, all the letters on the screen became white (higher in luminance than the background) for 0.5 second and then disappeared; at the same time, the feeder was illuminated. These changes signaled a "correct" response. With a probability of one in ten, correct responses were followed by access to food (mixed grain) for 3 seconds. After a correct response the screen remained blank white for 1.5 seconds; a new trial followed (*3*). If one of the nontarget keys was pecked, the letters disappeared, and after 1.5 seconds the target letter reappeared on the same key as before while black blocks (five by seven dot matrices) replaced the nontarget letters. This "correction" procedure was repeated until the target letter was pecked. Each session began with 25 trials in which the target letter was

0036-8075/82/1022-0397$01.00/0